Supplementary Information

Problems of dating spread on radiocarbon calibration curve plateaus: the 1620-1540 BC example and the dating of the Therasia olive shrub samples and Thera volcanic eruption

Sturt W. Manning

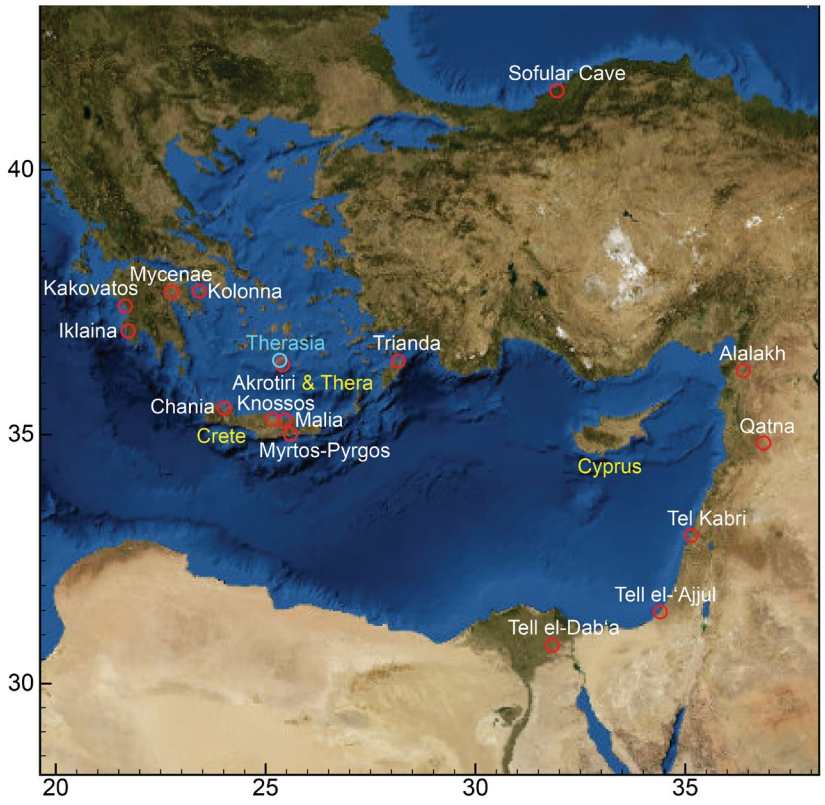

Figure S1. Map showing the Aegean-East Mediterranean region indicating the main locations or sites mentioned in the paper. Map created in OxCal 4.4.4 using USGS imagery.

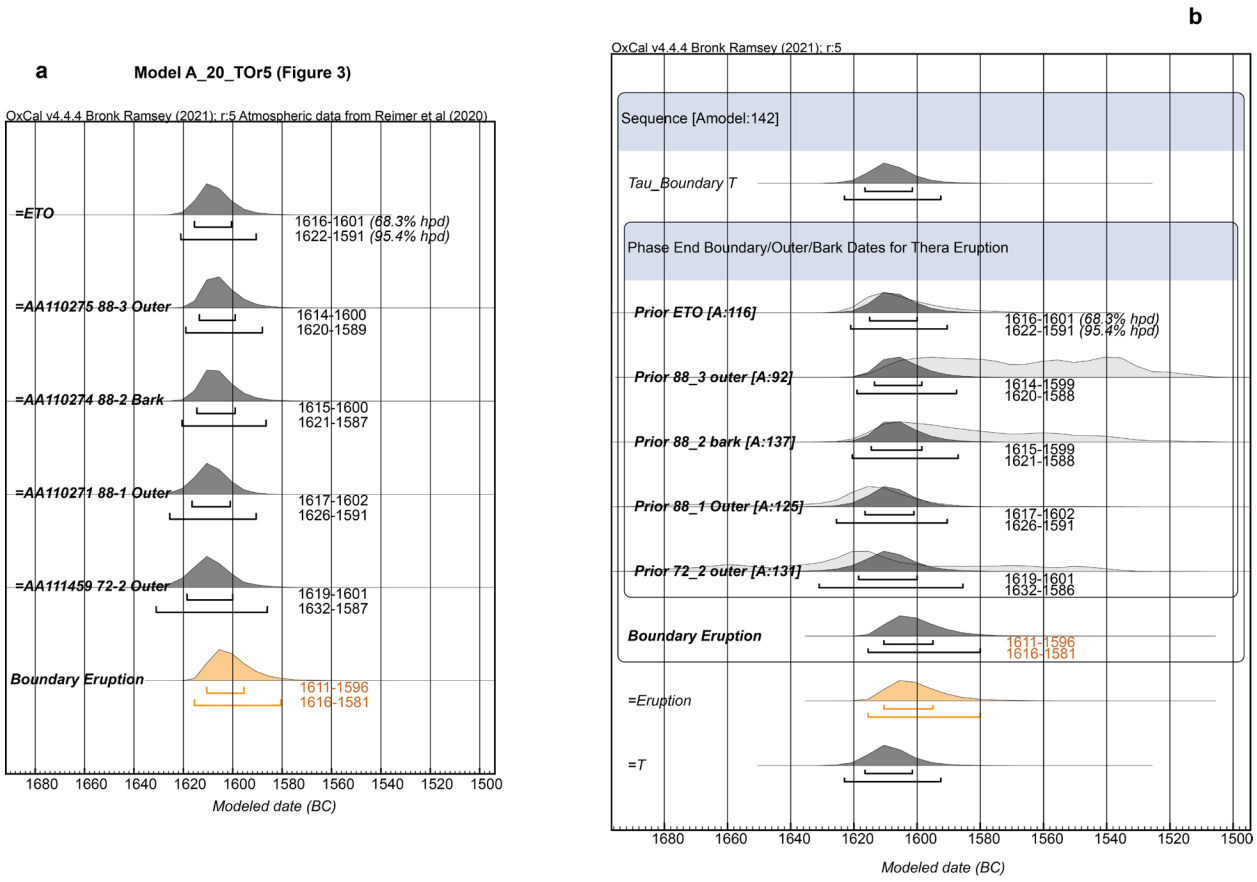

Figure S2. Comparison of the modeled probabilities and date ranges (68.3% and 95.4% highest posterior density, hpd) for the Boundary after the Friedrich et al. (2006; 2014) olive branch series, the outermost/bark elements dated for the four Therasia olive shrub samples, and then the modeled Boundary representing the approximate date of the Thera eruption using the model form described in the main text with this Phase modeled as an exponential distribution using a Tau_Boundary paired with a Boundary (see Model A_20_TOr5 shown in Figure 3). **a.** the probabilities and date ranges from the combined Model A_20_TOr5 as shown in Figure 3. **b.** the probabilities and date ranges if the initial Sequences for each sample/item are run separately and the probabilities for the relevant individual elements stored as Prior files and then the exponential model is run separately using these (with a time constant of 0-20 years as in Model A_20_TO5r in Figure 3). Although very minor variations occur between different model runs (as in all such model runs), the results are effectively identical. Data from OxCal 4.4.4 and IntCal20 with curve resolution set at 5 years.

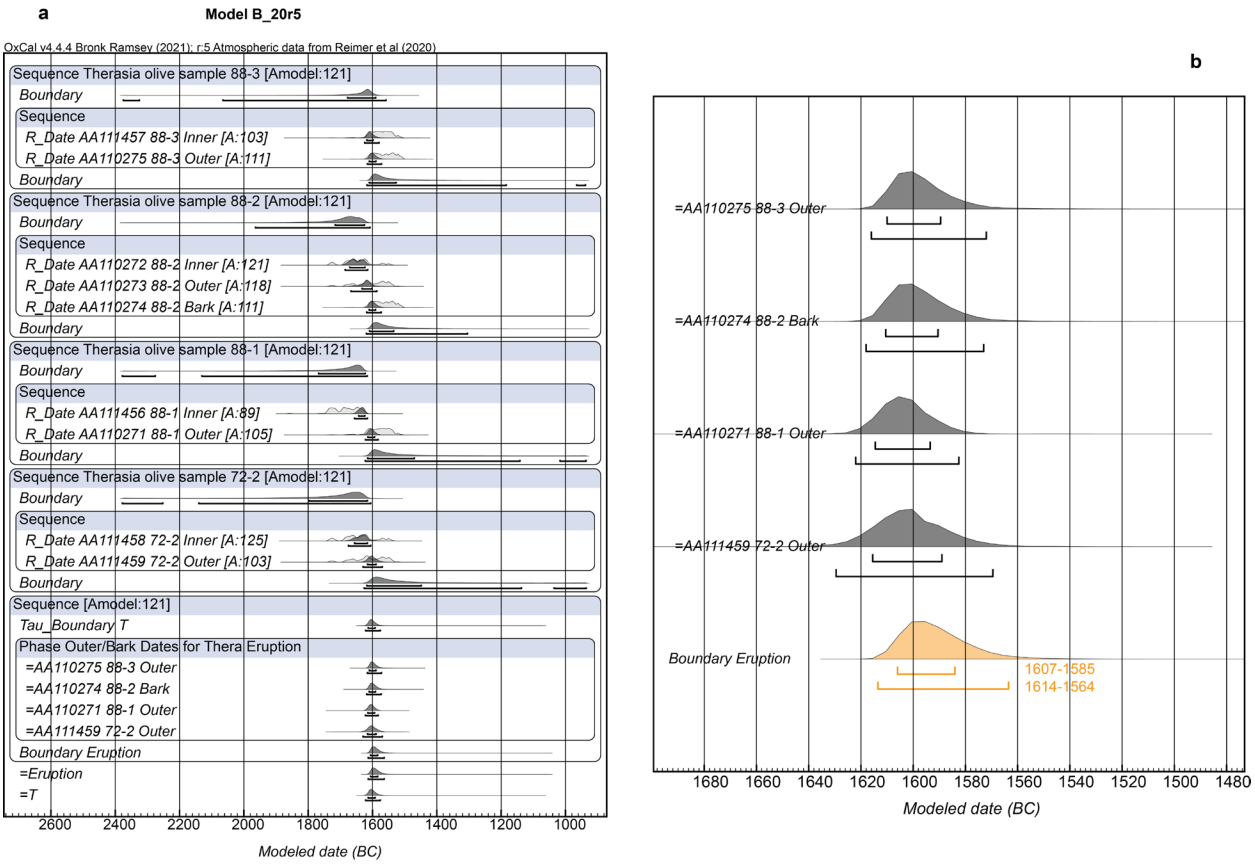

Figure S3. Model B_20r5. **a.** Model structure and results. Hollow, light-shaded, distributions show the non-modeled probability, the dark-shaded distributions show the modeled probability. The lines under the modeled distributions show the 68.3% and 95.4% hpd ranges. **b.** Details of the modeled probabilities for the four outer or bark samples from the Therasia olive shrub and for the Boundary "Eruption" that estimates the date the Therasia olive samples were collectively killed, and thus the date of the Thera volcanic eruption. Data from OxCal 4.4.4 and IntCal20 with curve resolution set at 5 years.

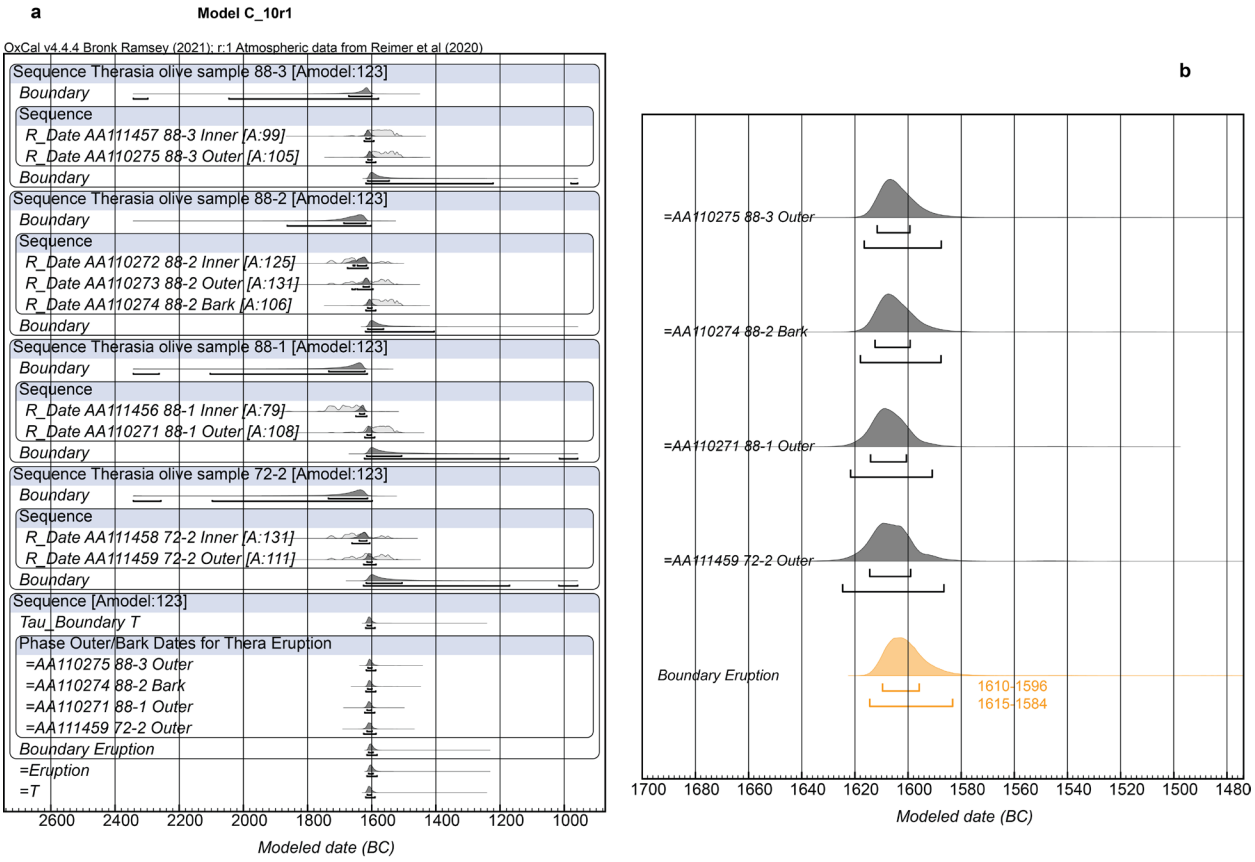

Figure S4. Model C_10r1. **a.** Model structure and results. Hollow, light-shaded, distributions show the non-modeled probability, the dark-shaded distributions show the modeled probability. The lines under the modeled distributions show the 68.3% and 95.4% hpd ranges. **b.** Details of the modeled probabilities for the four outer or bark samples from the Therasia olive shrub and for the Boundary "Eruption" that estimates the date the Therasia olive samples were collectively killed, and thus the date of the Thera volcanic eruption. Data from OxCal 4.4.4 and IntCal20 with curve resolution set at 1 year.

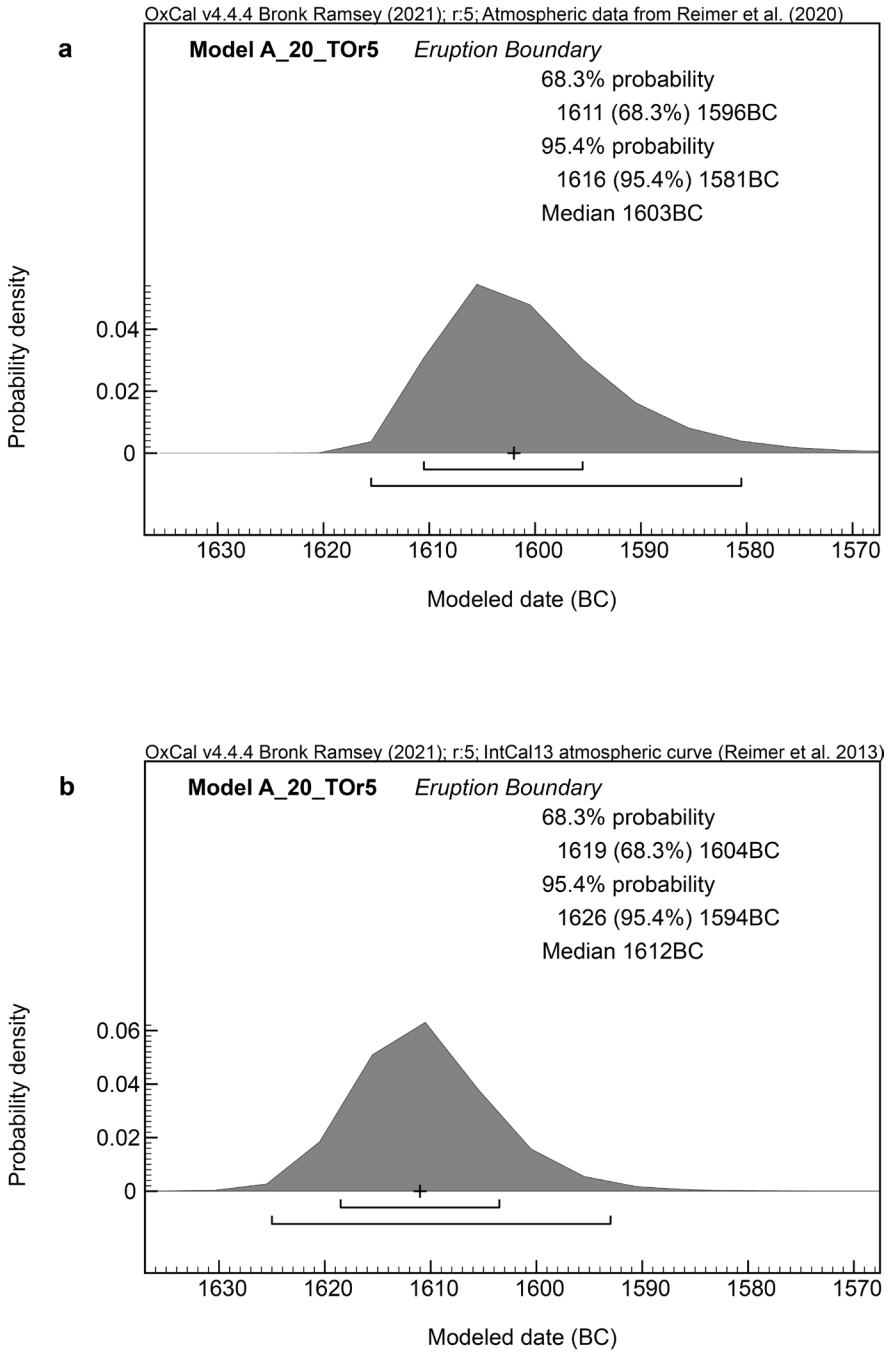

Figure S5. Comparison of the modeled Boundary representing the date of the Thera volcanic eruption from Model A_20_TOr5 (as shown in Figure 3) depending on radiocarbon calibration curve employed. **a.** Using the current IntCal20 radiocarbon calibration curve (as in Figure 3 and as reported for this model in Table 2). **b.** Using the previous IntCal13 radiocarbon calibration curve (Reimer et al. 2013). We can observe that the effect of the inclusion of many new data and the consequent revision of the calibration curve 1700-1500 BC, as included in IntCal20 (Reimer et al. 2020), is that the relevant dating probability is shifted around 10 calendar years to more recent ages (as observed by e.g. van der Plicht et al. 2020).

OxCal runfile for model used for Table 1 and Figure 1 (data from Pearson et al. 2023)

```
Options()
 {
  Resolution=5;
  Curve="intcal20.14c";
  kIterations=3000;
 };
 Plot()
 {
  Sequence("1A, 88-3 NO Boundaries")
  {
   R_Date("88-3 I",3314,23);
   R_Date("88-3 O",3297,23);
  };
  Sequence("1B, Therasia olive sample 88-3 - WITH Boundaries")
  {
   Boundary();
   Sequence()
   {
    R_Date("AA111457 88-3 Inner",3314,23);
    R_Date("AA110275 88-3 Outer",3297,23);
   };
   Boundary();
  };
  Sequence("2A, 88-2 NO Boundaries")
  {
   R_Date("88-2 I",3361,21);
   R_Date("88-2 O",3341,23);
   R_Date("88-2 B",3301,23);
  };
  Sequence("2B, Therasia olive sample 88-2 WITH Boundaries")
  {
   Boundary();
   Sequence()
   {
    R_Date("AA110272 88-2 Inner",3361,21);
    R_Date("AA110273 88-2 Outer",3341,23);
    R_Date("AA110274 88-2 Bark",3301,23);
   };
   Boundary();
  };
  Sequence("3A, 88-1 NO Boundaries")
  {
   R_Date("88-1 I",3398,21);
   R_Date("88-1 O",3320,22);
  };
  Sequence("3B, Therasia olive sample 88-1 WITH Boundaries")
  {
   Boundary();
   Sequence()
   {
    R_Date("AA111456 88-1 Inner",3398,21);
    R_Date("AA110271 88-1 Outer",3320,22);
   };
   Boundary();
  };
  Sequence("4A, 72-2 NO Boundaries")
  {
   R_Date("72-2 I",3358,23);
   R_Date("72-2 O",3342,24);
  };
  Sequence("4B, Therasia olive sample 72-2 WITH Boundaries")
```

```
  {
   Boundary();
   Sequence()
   {
    R_Date("AA111458 72-2 Inner",3358,23);
    R_Date("AA111459 72-2 Outer",3342,24);
   };
   Boundary();
  };
  Difference("D1A","88-3 O","88-3 I");
  Difference("D2A","88-2 B","88-2 I");
  Difference("D3A","88-1 O","88-1 I");
  Difference("D4A","72-2 O","72-2 I");
  Difference("D1B","AA110275 88-3 Outer","AA111457 88-3 Inner");
  Difference("D2B","AA110274 88-2 Bark","AA110272 88-2 Inner");
  Difference("D3B","AA110271 88-1 Outer","AA111456 88-1 Inner");
  Difference("D4B","AA111459 72-2 Outer","AA111458 72-2 Inner");
 };
```

OxCal runfile for Model A_20r1 in Figure 2

```
Options()
 {
  Resolution=1;
  Curve="intcal20.14c";
  kIterations=3000;
 };
 Plot()
 {
  Sequence("Therasia olive sample 88-3")
  {
   Boundary();
   Sequence()
   {
    R_Date("AA111457 88-3 Inner",3314,23);
    R_Date("AA110275 88-3 Outer",3297,23);
   };
   Boundary();
  };
  Sequence("Therasia olive sample 88-2")
  {
   Boundary();
   Sequence()
   {
    R_Date("AA110272 88-2 Inner",3361,21);
    R_Date("AA110273 88-2 Outer",3341,23);
    R_Date("AA110274 88-2 Bark",3301,23);
   };
   Boundary();
  };
  Sequence("Therasia olive sample 88-1")
  {
   Boundary();
   Sequence()
   {
    R_Date("AA111456 88-1 Inner",3398,21);
    R_Date("AA110271 88-1 Outer",3320,22);
   };
   Boundary();
  };
  Sequence("Therasia olive sample 72-2")
```

```
 {
  Boundary();
  Sequence()
  {
   R_Date("AA111458 72-2 Inner",3358,23);
   R_Date("AA111459 72-2 Outer",3342,24);
  };
  Boundary();
 };
 Sequence()
 {
  Tau_Boundary("T");
  Phase("Outer/Bark Dates for Thera Eruption")
  {
   Date("=AA110275 88-3 Outer");
   Date("=AA110274 88-2 Bark");
   Date("=AA110271 88-1 Outer");
   Date("=AA111459 72-2 Outer");
  };
  Boundary("Eruption");
 };
 Difference("D2","AA110275 88-3 Outer","AA111457 88-3 Inner",U(0,10));
 Difference("D3","AA110274 88-2 Bark","AA110272 88-2 Inner",U(0,79));
 Difference("D4","AA110271 88-1 Outer","AA111456 88-1 Inner",U(0,37));
 Difference("D5","AA111459 72-2 Outer","AA111458 72-2 Inner",U(0,50));
 Tau=(Eruption-T);
 Tau&=U(0,20);
};
```

OxCal runfile for Model A_20TOr5 in Figures 3 and 4 (note, as an example for other similar cases, the model version Model A_20TOr1 referred to in the main text and with results listed in Table 2 is the same except for changing `Resolution=5;` **to** `Resolution=1;`**)**

```
Options()
 {
  Resolution=5;
  Curve="intcal20.14c";
  kIterations=3000;
 };
 Plot()
 {
  Sequence()
  {
   Boundary("STO");
   Sequence()
   {
    R_Date("Hd-23599-24426 'rings' 1-13",3383,11);
    R_Date("Hd-23587 'rings' 14-37",3372,12);
    R_Date("Hd-23589 'rings' 38-59",3349,12);
    R_Date("Hd-23588-24402 'rings' 60-72",3331,10);
   };
   Boundary("ETO");
  };
  Sequence("Therasia olive sample 88-3")
  {
   Boundary();
   Sequence()
   {
    R_Date("AA111457 88-3 Inner",3314,23);
    R_Date("AA110275 88-3 Outer",3297,23);
   };
```

```
   Boundary();
  };
  Sequence("Therasia olive sample 88-2")
  {
   Boundary();
   Sequence()
   {
    R_Date("AA110272 88-2 Inner",3361,21);
    R_Date("AA110273 88-2 Outer",3341,23);
    R_Date("AA110274 88-2 Bark",3301,23);
   };
   Boundary();
  };
  Sequence("Therasia olive sample 88-1")
  {
   Boundary();
   Sequence()
   {
    R_Date("AA111456 88-1 Inner",3398,21);
    R_Date("AA110271 88-1 Outer",3320,22);
   };
   Boundary();
  };
  Sequence("Therasia olive sample 72-2")
  {
   Boundary();
   Sequence()
   {
    R_Date("AA111458 72-2 Inner",3358,23);
    R_Date("AA111459 72-2 Outer",3342,24);
   };
   Boundary();
  };
  Sequence()
  {
   Tau_Boundary("T");
   Phase("End Boundary/Outer/Bark Dates for Thera Eruption")
   {
    Date("=ETO");
    Date("=AA110275 88-3 Outer");
    Date("=AA110274 88-2 Bark");
    Date("=AA110271 88-1 Outer");
    Date("=AA111459 72-2 Outer");
   };
   Boundary("Eruption");
  };
  Difference("D1","ETO","STO",U(0,72));
  Difference("D2","AA110275 88-3 Outer","AA111457 88-3 Inner",U(0,10));
  Difference("D3","AA110274 88-2 Bark","AA110272 88-2 Inner",U(0,79));
  Difference("D4","AA110271 88-1 Outer","AA111456 88-1 Inner",U(0,37));
  Difference("D5","AA111459 72-2 Outer","AA111458 72-2 Inner",U(0,50));
  Tau=(Eruption-T);
  Tau&=U(0,20);
 };
```

Model A_20r1U (Table 2)

```
Options()
 {
  Resolution=1;
  Curve="intcal20.14c";
```

```
 kIterations=3000;
};
Plot()
{
 Sequence("Therasia olive sample 88-3")
 {
  Boundary();
  Sequence()
  {
   R_Date("AA111457 88-3 Inner",3314,23);
   R_Date("AA110275 88-3 Outer",3297,23);
  };
  Boundary();
 };
 Sequence("Therasia olive sample 88-2")
 {
  Boundary();
  Sequence()
  {
   R_Date("AA110272 88-2 Inner",3361,21);
   R_Date("AA110273 88-2 Outer",3341,23);
   R_Date("AA110274 88-2 Bark",3301,23);
  };
  Boundary();
 };
 Sequence("Therasia olive sample 88-1")
 {
  Boundary();
  Sequence()
  {
   R_Date("AA111456 88-1 Inner",3398,21);
   R_Date("AA110271 88-1 Outer",3320,22);
  };
  Boundary();
 };
 Sequence("Therasia olive sample 72-2")
 {
  Boundary();
  Sequence()
  {
   R_Date("AA111458 72-2 Inner",3358,23);
   R_Date("AA111459 72-2 Outer",3342,24);
  };
  Boundary();
 };
 Sequence()
 {
  Boundary("S");
  Phase("End Boundary/Outer/Bark Dates for Thera Eruption")
  {
   Date("=AA110275 88-3 Outer");
   Date("=AA110274 88-2 Bark");
   Date("=AA110271 88-1 Outer");
   Date("=AA111459 72-2 Outer");
  };
  Boundary("Eruption");
 };
 Difference("D2","AA110275 88-3 Outer","AA111457 88-3 Inner",U(0,10));
 Difference("D3","AA110274 88-2 Bark","AA110272 88-2 Inner",U(0,79));
 Difference("D4","AA110271 88-1 Outer","AA111456 88-1 Inner",U(0,37));
 Difference("D5","AA111459 72-2 Outer","AA111458 72-2 Inner",U(0,50));
 Difference("D6","Eruption","S",U(0,20));
};
```

Model B_20r5 (Table 2, Figure S3)

```
Options()
 {
  Resolution=5;
  Curve="intcal20.14c";
  kIterations=3000;
 };
 Plot()
 {
  Sequence("Therasia olive sample 88-3")
  {
   Boundary();
   Sequence()
   {
    R_Date("AA111457 88-3 Inner",3314,23);
    R_Date("AA110275 88-3 Outer",3297,23);
   };
   Boundary();
  };
  Sequence("Therasia olive sample 88-2")
  {
   Boundary();
   Sequence()
   {
    R_Date("AA110272 88-2 Inner",3361,21);
    R_Date("AA110273 88-2 Outer",3341,23);
    R_Date("AA110274 88-2 Bark",3301,23);
   };
   Boundary();
  };
  Sequence("Therasia olive sample 88-1")
  {
   Boundary();
   Sequence()
   {
    R_Date("AA111456 88-1 Inner",3398,21);
    R_Date("AA110271 88-1 Outer",3320,22);
   };
   Boundary();
  };
  Sequence("Therasia olive sample 72-2")
  {
   Boundary();
   Sequence()
   {
    R_Date("AA111458 72-2 Inner",3358,23);
    R_Date("AA111459 72-2 Outer",3342,24);
   };
   Boundary();
  };
  Sequence()
  {
   Tau_Boundary("T");
   Phase("Outer/Bark Dates for Thera Eruption")
   {
    Date("=AA110275 88-3 Outer");
    Date("=AA110274 88-2 Bark");
    Date("=AA110271 88-1 Outer");
    Date("=AA111459 72-2 Outer");
```

```
   };
   Boundary("Eruption");
  };
  Difference("D2","AA110275 88-3 Outer","AA111457 88-3 Inner",N(8,2));
  Difference("D3","AA110274 88-2 Bark","AA110272 88-2 Inner",N(59,20));
  Difference("D4","AA110271 88-1 Outer","AA111456 88-1 Inner",N(28,9));
  Difference("D5","AA111459 72-2 Outer","AA111458 72-2 Inner",N(37,12));
  Tau=(Eruption-T);
  Tau&=U(0,20);
 };
```

Model C_10r1 (Table 2, Figure S4)

```
Options()
 {
  Resolution=1;
  Curve="intcal20.14c";
  kIterations=3000;
 };
 Plot()
 {
  Sequence("Therasia olive sample 88-3")
  {
   Boundary();
   Sequence()
   {
    R_Date("AA111457 88-3 Inner",3314,23);
    R_Date("AA110275 88-3 Outer",3297,23);
   };
   Boundary();
  };
  Sequence("Therasia olive sample 88-2")
  {
   Boundary();
   Sequence()
   {
    R_Date("AA110272 88-2 Inner",3361,21);
    R_Date("AA110273 88-2 Outer",3341,23);
    R_Date("AA110274 88-2 Bark",3301,23);
   };
   Boundary();
  };
  Sequence("Therasia olive sample 88-1")
  {
   Boundary();
   Sequence()
   {
    R_Date("AA111456 88-1 Inner",3398,21);
    R_Date("AA110271 88-1 Outer",3320,22);
   };
   Boundary();
  };
  Sequence("Therasia olive sample 72-2")
  {
   Boundary();
   Sequence()
   {
    R_Date("AA111458 72-2 Inner",3358,23);
    R_Date("AA111459 72-2 Outer",3342,24);
   };
   Boundary();
```

```
 };
 Sequence()
 {
  Tau_Boundary("T");
  Phase("Outer/Bark Dates for Thera Eruption")
  {
   Date("=AA110275 88-3 Outer");
   Date("=AA110274 88-2 Bark");
   Date("=AA110271 88-1 Outer");
   Date("=AA111459 72-2 Outer");
  };
  Boundary("Eruption");
 };
 Difference("D2","AA110275 88-3 Outer","AA111457 88-3 Inner",N(6.5,2));
 Difference("D3","AA110274 88-2 Bark","AA110272 88-2 Inner",N(40,20));
 Difference("D4","AA110271 88-1 Outer","AA111456 88-1 Inner",N(19,9));
 Difference("D5","AA111459 72-2 Outer","AA111458 72-2 Inner",N(25,12));
 Tau=(Eruption-T);
 Tau&=U(0,10);
};
```

OxCal runfile for the Thera eruption dating model for Figure 6

```
Options()
 {
  Resolution=5;
  Curve="intcal20.14c";
  kIterations=3000;
 };
 Plot()
 {
  Sequence()
  {
   Boundary("STO");
   Sequence()
   {
    R_Date("Hd-23599-24426 'rings' 1-13",3383,11);
    R_Date("Hd-23587 'rings' 14-37",3372,12);
    R_Date("Hd-23589 'rings' 38-59",3349,12);
    R_Date("Hd-23588-24402 'rings' 60-72",3331,10);
   };
   Boundary("ETO");
  };
  Sequence("Therasia olive sample 88-3")
  {
   Boundary();
   Sequence()
   {
    R_Date("AA111457 88-3 Inner",3314,23);
    R_Date("AA110275 88-3 Outer",3297,23);
   };
   Boundary();
  };
  Sequence("Therasia olive sample 88-2")
  {
   Boundary();
   Sequence()
   {
    R_Date("AA110272 88-2 Inner",3361,21);
    R_Date("AA110273 88-2 Outer",3341,23);
    R_Date("AA110274 88-2 Bark",3301,23);
   };
```

```
   Boundary();
  };
  Sequence("Therasia olive sample 88-1")
  {
   Boundary();
   Sequence()
   {
    R_Date("AA111456 88-1 Inner",3398,21);
    R_Date("AA110271 88-1 Outer",3320,22);
   };
   Boundary();
  };
  Sequence("Therasia olive sample 72-2")
  {
   Boundary();
   Sequence()
   {
    R_Date("AA111458 72-2 Inner",3358,23);
    R_Date("AA111459 72-2 Outer",3342,24);
   };
   Boundary();
  };
  Sequence()
  {
   Tau_Boundary("T");
   Phase("End Boundary/Outer/Bark Dates for Thera Eruption")
   {
    Date("=ETO");
    Date("=AA110275 88-3 Outer");
    Date("=AA110274 88-2 Bark");
    Date("=AA110271 88-1 Outer");
    Date("=AA111459 72-2 Outer");
   };
   Boundary("Eruption");
  };
  Difference("D1","ETO","STO",U(0,72));
  Difference("D2","AA110275 88-3 Outer","AA111457 88-3 Inner",U(0,10));
  Difference("D3","AA110274 88-2 Bark","AA110272 88-2 Inner",U(0,79));
  Difference("D4","AA110271 88-1 Outer","AA111456 88-1 Inner",U(0,37));
  Difference("D5","AA111459 72-2 Outer","AA111458 72-2 Inner",U(0,50));
  Tau=(Eruption-T);
  Tau&=LnN(ln(3),ln(2));
 };

//In Options, change Resolution=5; to Resolution=1; for the 1-year resolution model
```

OxCal runfiles for the Thera eruption TAQ model for Figure 7. Separate Sequences were run for each site. The relevant TAQ Boundary or Date query was then saved as a Prior file and the model shown in Figure 7 was run using these Prior files. An approximate growing season offset for relevant species in the southern Levant and Egypt (see Manning et al. 2020b; 2020c) is applied (only) to the series from Tell el-‘Ajjul and Tell el-Dab‘a, using the approach and values as described in Höflmayer and Manning (2022).

```
Options()
 {
  Resolution=1;
  Curve="intcal20.14c";
  kIterations=3000;
 };
```

```
 Plot()
 {
  Outlier_Model("General",T(5),U(0,4),"t");
  Outlier_Model("SSimple",N(0,2),0,"s");
  Sequence("Kolonna, Aegina")
  {
   //S = short-lived plant material, B = animal bone, C = charcoal (apparently not
very long-lived, T = wood twig, so shorter-lived).
   //Wild et al. 2010 model
   Boundary("Begin E");
   Phase("Phase E")
   {
    Sequence()
    {
     Combine("fire destruction")
     {
      Outlier ("General",0.05);
      R_Date("VERA-2678 S",3724,35)
      {
       Outlier("SSimple",0.05);
      };
      R_Date("VERA-2680 S",3722,35)
      {
       Outlier("SSimple",0.05);
      };
      R_Date("VERA-2681 S",3739,35)
      {
       Outlier("SSimple",0.05);
      };
      R_Date("VERA-2679 S",3761,35)
      {
       Outlier("SSimple",0.05);
      };
      R_Date("VRI-0395 C",3670,90)
      {
       Outlier("SSimple",0.05);
      };
      R_Date("HV-5841 C",3625,65)
      {
       Outlier("SSimple",0.05);
      };
      R_Date("VERA-2682 S",3712,35)
      {
       Outlier("SSimple",0.05);
      };
      R_Date("VERA-2683 S",3721,35)
      {
       Outlier("SSimple",0.05);
      };
      R_Date("HV-5840 C",3820,65)
      {
       Outlier("SSimple",0.05);
      };
     };
     R_Date("VERA-4641 B",3759,35)
     {
      Outlier ("General",0.05);
     };
    };
    R_Date("VERA-2688 B",3698,33)
    {
     Outlier ("General",0.05);
    };
```

```
};
Boundary("Transition E/F");
Phase("Phase F")
{
 R_Date("VERA-2692 B",3704,36)
 {
  Outlier ("General",0.05);
 };
};
Boundary("Transition F/G");
Phase("Phase G")
{
 Sequence("Sequence 1")
 {
  R_Date("VERA-4640 B",3800,44)
  {
   Outlier ("General",0.05);
  };
  R_Date("VERA-4639 B",3809,32)
  {
   Outlier ("General",0.05);
  };
 };
 R_Date("VERA-4638 B",3646,32)
 {
  Outlier ("General",0.05);
 };
 R_Date("VERA-4281 S",3740,36)
 {
  Outlier ("General",0.05);
 };
 R_Date("VERA-4282 S",3711,34)
 {
  Outlier ("General",0.05);
 };
 R_Date("VERA-4283 S",3780,37)
 {
  Outlier ("General",0.05);
 };
};
Boundary("Transition G/H");
Phase("Phase H")
{
 Sequence("Sequence 2")
 {
  R_Date("VERA-4637 B",3643,30)
  {
   Outlier ("General",0.05);
  };
  R_Date("VERA-4636 B",3628,30)
  {
   Outlier ("General",0.05);
  };
 };
 Sequence("Sequence 3")
 {
  R_Date("VERA-4280 S",3724,39)
  {
   Outlier ("General",0.05);
  };
  R_Date("VERA-4279 S",3718,38)
  {
   Outlier ("General",0.05);
```

```
  };
 };
 R_Date("VERA-2687",3694 B,35)
 {
  Outlier ("General",0.05);
 };
};
Boundary("Transition H/I");
Phase("Phase I")
{
 Sequence()
 {
  Phase("before Minoan layer")
  {
   R_Date("VERA-4634 B",3544,37)
   {
    Outlier ("General",0.05);
   };
   R_Date("VERA-4278 S",3522,38)
   {
    Outlier ("General",0.05);
   };
  };
  Combine("Minoan layer")
  {
   Outlier ("General",0.05);
   R_Date("VERA-4038 S",3506,34)
   {
    Outlier("SSimple",0.05);
   };
   R_Date("VERA-4576 B",3482,37)
   {
    Outlier("SSimple",0.05);
   };
   R_Date("VERA-4575 B",3537,36)
   {
    Outlier("SSimple",0.05);
   };
   R_Date("VERA-4578 B",3501,39)
   {
    Outlier("SSimple",0.05);
   };
   R_Date("VERA-4579 B",3526,38)
   {
    Outlier("SSimple",0.05);
   };
   R_Date("VERA-4580 B",3506,33)
   {
    Outlier("SSimple",0.05);
   };
   R_Date("VERA-4276 S",3506,37)
   {
    Outlier("SSimple",0.05);
   };
   R_Date("VERA-4275 S",3544,38)
   {
    Outlier("SSimple",0.05);
   };
  };
  R_Date("VERA-4577 B",3458,39)
  {
   Outlier ("General",0.05);
  };
```

```
 };
};
Boundary("Transition I/J");
Phase("Phase J = MHIII")
{
 Sequence()
 {
  Combine()
  {
   Outlier ("General",0.05);
   R_Date("VERA-4571 B",3469,38)
   {
    Outlier("SSimple",0.05);
   };
   R_Date("VERA-4574 B",3430,39)
   {
    Outlier("SSimple",0.05);
   };
   R_Date("VERA-4573 B",3485,36)
   {
    Outlier("SSimple",0.05);
   };
  };
  Phase()
  {
   R_Date("VERA-4572 B",3407,38)
   {
    Outlier ("General",0.05);
   };
   R_Date("VERA-4570 B",3428,36)
   {
    Outlier ("General",0.05);
   };
  };
 };
};
Boundary("Kolonna Transition J/K");
Phase("Phase K - LHI")
{
 Sequence()
 {
  R_Date("VERA-4633 B",3333,29)
  {
   Outlier ("General",0.05);
  };
  R_Date("VERA-4632 B",3356,36)
  {
   Outlier ("General",0.05);
  };
  R_Date("VERA-4631 B",3349,36)
  {
   Outlier ("General",0.05);
  };
 };
};
Boundary("Kolonna Transition K/L");
Phase("Phase L - LHII")
{
 R_Date("VERA-4630 B",3313,48)
 {
  Outlier ("General",0.05);
 };
 Date("Kolonna LHII");
```

```
   };
   Boundary("End Kolonna L: End LHII");
   Boundary("Begin Kolonna M: LHIIIA");
   Phase("Phase M - LHIIIA")
   {
    Combine()
    {
     Outlier ("General",0.05);
     R_Date("VERA-4284 S",3044,35)
     {
      Outlier("SSimple",0.05);
     };
     R_Date("VERA-4582 T",2986,33)
     {
      Outlier("SSimple",0.05);
     };
     R_Date("VERA-4285 S",3040,37)
     {
      Outlier("SSimple",0.05);
     };
    };
   };
   Boundary("End Phase M");
  };
 };


Options()
 {
  Resolution=1;
  Curve="intcal20.14c";
  kIterations=3000;
 };
 Plot()
 {
  Outlier_Model("General",T(5),U(0,4),"t");
  Delta_R("Egypt",12,5);
  Sequence("Tell el-Ajjul")
  {
   //Data: Fisher (2009). Pumice appears in both H5 sub-phases; Thera eruption
therefore either before H5 (i.e. H6) or at latest by early H5 (H5B) (Fisher 2009).
Thus the Boundary Transition H6 to H5 is the plausible TAQ for the Thera eruption.
Assume approximate growing season offset applies of Delta_R 12,5 for this southern
Levant locus (same basis as Tell el-Daba, see Höflmayer and Manning 2022).
   Boundary("Ajjul Start");
   Phase("H6")
   {
    R_Date("VERA-1905",3310,35)
    {
     Outlier("General",0.05);
    };
    R_Date("VERA-1904",3310,30)
    {
     Outlier("General",0.05);
    };
   };
   Boundary("Ajjul Transition H6 to H5");
   Phase("H5")
   {
    R_Date("VERA-1907",3280,35)
    {
     Outlier("General",0.05);
    };
```

```
    R_Date("VERA-1906",3260,35)
    {
     Outlier("General",0.05);
    };
    R_Date("VERA-1909",3285,35)
    {
     Outlier("General",0.05);
    };
    R_Date("VERA-1901",3230,30)
    {
     Outlier("General",0.05);
    };
   };
   Boundary("Ajjul Transition H5 to H4-3");
   Phase("H4-3")
   {
    R_Date("VERA-1902",3295,40)
    {
     Outlier("General",0.05);
    };
    R_Date("VERA-1910",3250,30)
    {
     Outlier("General",0.05);
    };
   };
   Boundary("Ajjul End");
  };
 };


Options()
 {
  Resolution=1;
  Curve="intcal20.14c";
  kIterations=3000;
 };
 Plot( )
 {
  Outlier_Model("General",T(5),U(0,4),"t");
  //Model after Kutchera et al. (2012) as revised and with approximate Egypt growing
offset allowance in Höflmayer and Manning (2022). The underscore _ indicates this
Delta_R adjusted model in Höflmayer and Manning (2022). Delta_R 19,5 where 14C
>=3450BP and 12,5 where 14C <3450BP (see Höflmayer and Manning 2022).
  Delta_R("Egypt1",19,5);
  Label("_Samples associated with particular boundaries:");
  R_Date("_F to E3, associated with VERA-3643 **)",3450,26)
  {
   Outlier("General", 0.05);
  };
  Delta_R("Egypt AMS1",12,5);
  R_Date("_D/3 to D/2, associated with VERA-3645 **)",3351,38)
  {
   Outlier("General", 0.05);
  };
  Label(" ");
  Delta_R("Egypt2",19,5);
  Sequence("_Tell el-Daba")
  {
   Boundary("_Start");
   Phase("_N/2-3")
   {
    R_Date("_VERA-2900 seeds, Lolium type",3755,26)
    {
```

```
  Outlier("General", 0.05);
 };
 R_Date("_VERA-3641 seeds, Lolium type",3739,38)
 {
  Outlier("General", 0.05);
 };
 R_Date("_VERA-2901 seeds, Poaceae",3725,30)
 {
  Outlier("General",0.05);
 };
};
Boundary("_Transition N/2-3 to N/1");
Phase("_N/1")
{
 R_Date("_VERA-2619 seed, Lolium type, Poaceae",3697,37)
 {
  Outlier("General", 0.05);
 };
 R_Date("_VERA-2620 seed, Lolium type, Poaceae",3688,36)
 {
  Outlier("General",0.05);
 };
};
Boundary("_Transition N/1 to M");
Phase("_M")
{
 R_Date("_VERA-2631 seeds, Cerealia, Lolium type",3643,35)
 {
  Outlier("General",0.05);
 };
};
Boundary("_Transition M to L *)");
Boundary("_Transition L to K *)");
Boundary("_Transition K to I *)");
Boundary("_I to H *)");
Phase("_H")
{
 R_Date("_VERA-2618 seed, Lolium type",3593,34)
 {
  Outlier("General",0.05);
 };
 R_Date("_VERA-3639 seeds, Lolium type",3553,25)
 {
  Outlier("General",0.05);
 };
 R_Date("_OxA-15951 seeds, Lolium type",3522,32)
 {
  Outlier("General",0.05);
 };
 R_Date("_OxA-15952 seeds, Lolium type",3577,32)
 {
  Outlier("General",0.05);
 };
 R_Date( "_VERA-3638 seeds, Lolium type",3522,37)
 {
  Outlier("General",0.05);
 };
};
Boundary("_Transition H to G/4");
Phase("_G/4")
{
 R_Date("_VERA-2899 seeds, Poaceae",3591,26)
 {
```

```
  Outlier("General", 0.05);
 };
 R_Date("_VERA-3640 seeds, Lolium type",3530,38)
 {
  Outlier("General",0.05);
 };
 R_Date("_OxA-15956 seeds, Lolium type",3504,32)
 {
  Outlier("General",0.05);
 };
 R_Date("_OxA-15954 seeds, Lolium type",3532,34)
 {
  Outlier("General",0.05);
 };
};
Boundary("_Transition G/4 to G/1-3");
Phase("_G/1-3")
{
 R_Date("_VERA-2624 seeds, Hordeum vulgare, Lolium type",3530,34)
 {
  Outlier("General",0.05);
 };
 R_Date("_VERA-2622 seeds, Lolium type, Poaceae",3481,36)
 {
  Outlier("General",0.05);
 };
 R_Date("_VERA-2623 seeds, Triticum dicoccum",3466,39)
 {
  Outlier("General",0.05);
 };
 Delta_R("Egypt AMS2",12,5);
 R_Date("_VERA-3642 seeds, Lolium type, Poaceae",3447,25)
 {
  Outlier("General",0.05);
 };
};
Boundary("_Transition G/1-3 to F");
Delta_R("Egypt3",19,5);
Phase("_F")
{
 R_Date("_VERA-2898 seeds, Lolium type, Phalaris/Cynodon sp.",3505,27)
 {
  Outlier("General",0.05);
 };
 R_Date("_VERA-2625 seeds, Lolium sp., Lolium type, Lolium/Bromus sp.",3467,35)
 {
  Outlier("General",0.05);
 };
};
Boundary("=_F to E3, associated with VERA-3643 **)");
Phase("_E/3")
{
 R_Date("_VERA-2897 seeds, Hordeum vulgare",3525,26)
 {
  Outlier("General",0.05);
 };
};
Boundary("_Transition E/3 to E/2");
Delta_R("Egypt AMS3",12,5);
Phase("_E/2")
{
 R_Date("_VERA-3637 seeds, Lolium type",3415,26)
 {
```

```
  Outlier("General",0.05);
 };
};
Boundary("_Transition E/2 to E/1");
Phase("_E/1")
{
 R_Date("_VERA-3618 seeds, Cerealia",3436,35)
 {
  Outlier("General",0.05);
 };
 R_Date("_OxA-15949 seeds, Cerealia",3437,30)
 {
  Outlier("General",0.05);
 };
 Delta_R("Egypt4",19,5);
 R_Date("_OxA-15948 seeds, Cerealia",3511,32)
 {
  Outlier("General",0.05);
 };
 Delta_R("Egypt AMS4",12,5);
 R_Date("_VERA-3636 seeds, Lolium type",3449,26)
 {
  Outlier("General",0.05);
 };
 R_Date("_VERA-3617 seeds, Poaceae",3422,35)
 {
  Outlier("General",0.05);
 };
 R_Date("_VERA-2626 seed, Lolium type, Lolium/Bromus/Agropyron sp",3389,36)
 {
  Outlier("General",0.05);
 };
};
Boundary("_Transition E/1 to D/3");
Phase("_D/3")
{
 R_Date("_VERA-3033 seed, Cerealia",3480,28)
 {
  Outlier("General",0.05);
 };
 R_Date("_VERA-2896 seeds, Poaceae",3428,37)
 {
  Outlier("General",0.05);
 };
 R_Date("_VERA-2895 seed, Lolium type",3426,26)
 {
  Outlier("General",0.05);
 };
 R_Date("_VERA-3619 seeds, Lolium type",3396,34)
 {
  Outlier("General",0.05);
 };
 R_Date("_VERA-2629 seeds, Lolium type, Poaceae",3384,30)
 {
  Outlier("General",0.05);
 };
 R_Date("_VERA-3620 seeds, Lolium type",3377,33)
 {
  Outlier("General",0.05);
 };
};
Boundary("=_D/3 to D/2, associated with VERA-3645 **)");
Phase("_D/2")
```

```
{
 R_Date("_VERA-3621 seeds, Lolium type",3354,26)
 {
  Outlier("General",0.05);
 };
 R_Date("_OxA-15953 seeds, Lolium type",3392,31)
 {
  Outlier("General",0.05);
 };
 Delta_R("Egypt5",19,5);
 R_Date("_OxA-15901 seeds, Lolium type",3479,33)
 {
  Outlier("General",0.05);
 };
 Delta_R("Egypt AMS5",12,5);
 R_Date("_VERA-3622 seeds, Poaceae",3394,36)
 {
  Outlier("General",0.05);
 };
 R_Date("_VERA-2627 seed, Lolium type",3390,34)
 {
  Outlier("General",0.05);
 };
 R_Date("_VERA-2628 seed, Triticum sp., Poaceae",3359,34)
 {
  Outlier("General",0.05);
 };
 R_Date("_VERA-3616 seeds, Poaceae",3337,44)
 {
  Outlier("General",0.05);
 };
};
Boundary("_Transition D/2 to D/1");
Phase("_D/1")
{
 R_Date("_VERA-3032 seed, Lolium type",3314,36)
 {
  Outlier("General",0.05);
 };
};
Boundary("_Transition D/1 to C/2-3");
Phase("_C/2-3")
{
 Sequence("_for sample exclusively in C/2")
 {
  Boundary("_start of C/2 *)");
  Phase("_C/2")
  {
   R_Date("_VERA-3031 seeds, Lolium type",3414,35)
   {
    Outlier("General", 0.05);
   };
  };
 };
 R_Date("_VERA-3725 seed, Lolium type",3336,29)
 {
  Outlier("General",0.05);
 };
 R_Date("_VERA-3724 seeds, Lolium type",3320,29)
 {
  Outlier("General",0.05);
 };
 R_Date("_OxA-15959 seeds, Lolium type",3296,31)
```

```
    {
     Outlier("General",0.05);
    };
    R_Date("_OxA-15957 seeds, Lolium type",3322,31)
    {
     Outlier("General",0.05);
    };
   };
   Boundary("End");
  };
 };


Options()
 {
  Resolution=1;
  Curve="intcal20.14c";
  kIterations=3000;
 };
 Plot()
 {
  //Data: Cosmopoulos et al. (2019)
  Outlier_Model("General",T(5),U(0,4),"t");
  Sequence ("Iklainia LHIIA-IIB or LHII and then LHIIB/IIIA dates on Short/Shorter-
Lived Samples Only")
  {
   Boundary("TAQ for Start Iklaina LHII");
   Phase ("LHIIA-IIB or LHII or LHIIB/IIIA SL")
   {
    R_Date("AA110766 Bos R. mid metararsus LHIIA-IIB",3231,27)
    {
     Outlier ("General",0.05);
    };
    R_Date("AA110769 Cervus prox. R. femur LHIIA-IIB",3303,28)
    {
     Outlier ("General",0.05);
    };
    R_Date("AA110754 Cereal indeterm. LHII",3272,40)
    {
     Outlier ("General",0.05);
    };
   };
   Boundary("Transition LHIIA-IIB or LHII to LHIIB/IIIA1");
   R_Date("AA110757 Cereal indet. seed LHIIB/IIIA1",3217,22)
   {
    Outlier ("General",0.05);
   };
   Boundary("Transition Iklaina LHIIB/LHIIIA1 to LHIIIA2/IIIB");
   R_Date("AA110767 Sus R. distal humerus LHIIIA1-IIIA2",3172,27)
   {
    Outlier ("General",0.05);
   };
   Boundary("Transition LHIIIA1/IIIA2 to LHIIIA2/IIIB");
   Phase ("LHIIIA2/IIIB")
   {
    R_Date("AA110771 Ovis R. mid humerus LHIIIB",3068,25)
    {
     Outlier ("General",0.05);
    };
    R_Date("AA110758 Vicia faba LHIIIB",3034,21)
    {
     Outlier ("General",0.05);
    };
```

```
    R_Date("AA110765 Fig LHIIIA2/IIIB",3095,39)
    {
     Outlier ("General",0.05);
    };
    R_Date("AA110761 Hordeum vulgare LHIIIA2/LHIIIB",3033,20)
    {
     Outlier ("General",0.05);
    };
   };
   Boundary();
  };
 };
 //NOTE: I do not include AA110768 as it is stated to be "LHI-II" and so it is not
clear if a TAQ for Thera Eruption, ditto likely pre-Thera eruption AA110772 from a MH-
LHI/II context, nor AA110759 or AA11076 nor AA110764 as all wood samples, Quercus sp.,
and so have possible in-built age issues. For data and stratigraphic associations, see
Cosmopoulos et al. 2019.


Options()
 {
  Resolution=1;
  Curve="intcal20.14c";
  kIterations=3000;
 };
 Plot()
 {
  //Data: Eder and Hadzi-Spiliopoulou (2021)
  Outlier_Model("General",T(5),U(0,4),"t");
  Sequence("Kakovatos LHIIA to LHIIB, all short-lived samples")
  {
   Boundary("Start LHIIA Kakovatos");
   Phase ("LHIIA Kakovatos")
   {
    R_Date("MAM-27561 cattle bone",3330,26)
    {
     Outlier ("General",0.05);
    };
    R_Date("MAMS-27562 sheep/goat bone",3259,25)
    {
     Outlier ("General",0.05);
    };
   };
   Boundary("LHIIA/LHIIB Transition Kakavatos");
   Phase("LHIIB Kakavatos")
   {
    R_Date("MAMS-18178 Fig",3175,17)
    {
     Outlier ("General",0.05);
    };
    R_Date("MAMS-18181 Carbonised figs",3217,17)
    {
     Outlier ("General",0.05);
    };
    R_Date("MAMS-24249 Grain",3241,24)
    {
     Outlier ("General",0.05);
    };
    R_Date("DEM-1996 Carbonised figs",3179,30)
    {
     Outlier ("General",0.05);
    };
    R_Date("MAMS-24250 Barley",3261,24)
```

```
    {
     Outlier ("General",0.05);
    };
    R_Date("MAMS-18177 Carbonised fig",3166,18)
    {
     Outlier ("General",0.05);
    };
    R_Date("MAMS-24251 Grain",3226,24)
    {
     Outlier ("General",0.05);
    };
   };
   Boundary();
  };
 };


Options()
 {
  Resolution=1;
  Curve="intcal20.14c";
  kIterations=3000;
 };
 Plot()
 {
  //Data: Manning (2009)
  Outlier_Model("General",T(5),U(0,4),"t");
  Sequence()
  {
   Boundary("Start Chania Late LMIB");
   Phase("Chania Late LMIB")
   {
    R_Date("OxA-2517 Pisum sativum",3380,80)
    {
     Outlier ("General",0.05);
    };
    R_Date("OxA-2518 Vicia faba",3340,80)
    {
     Outlier ("General",0.05);
    };
    R_Date("OxA-2646 Hordeum sp.",3315,70)
    {
     Outlier ("General",0.05);
    };
    R_Date("OxA-2647 charred seed",3150,70)
    {
     Outlier ("General",0.05);
    };
    R_Date("OxA-10320 Vicia faba",3208,26)
    {
     Outlier ("General",0.05);
    };
    R_Date("OxA-10321 Horedeum sp.",3268,27)
    {
     Outlier ("General",0.05);
    };
    R_Date("OxA-10322 Pisum sativum",3338,26)
    {
     Outlier ("General",0.05);
    };
    R_Date("OxA-10323 charred seed",3253,25)
    {
     Outlier ("General",0.05);
```

```
  };
 };
 Boundary();
};
Sequence("Late LMIB to LMIB Final")
{
 Boundary("Start Myrtos-Pyrgos Late LMIB");
 Phase("Myrtos-Pyrgos (LMIB Late) Destruction")
 {
  R_Date("OxA-3187 Hordeum sp.",3230,70)
  {
   Outlier ("General",0.05);
  };
  R_Date("OxA-3188 Hordeum sp.",3200,70)
  {
   Outlier ("General",0.05);
  };
  R_Date("OxA-3189 Vicia ervilia",3270,70)
  {
   Outlier ("General",0.05);
  };
  R_Date("OxA-3225 Vicia ervilia",3160,80)
  {
   Outlier ("General",0.05);
  };
  R_Date("OxA-10324 Hordeum sp.",3270,26)
  {
   Outlier ("General",0.05);
  };
  R_Date("OxA-10325 Vicia ervilia",3228,26)
  {
   Outlier ("General",0.05);
  };
  R_Date("OxA-10326 Vicia ervilia",3227,25)
  {
   Outlier ("General",0.05);
  };
  R_Date("OxA-10411 Hordeum sp.",3150,40)
  {
   Outlier ("General",0.05);
  };
 };
 Boundary("Transition LMIB Late to LMIB Final");
 Phase("Mochlos (LMIB Final) Destruction")
 {
  R_Date("Beta-85991 Olea europaea",3240,50)
  {
   Outlier ("General",0.05);
  };
  R_Date("Beta-85992 Olea europaea",3180,40)
  {
   Outlier ("General",0.05);
  };
  R_Date("Beta-115890 Olea europaea",3170,60)
  {
   Outlier ("General",0.05);
  };
  R_Date("Beta-129765 Olea europaea",3220,40)
  {
   Outlier ("General",0.05);
  };
  R_Date("Beta-151768 Olea europaea",3270,40)
  {
```

```
     Outlier ("General",0.05);
    };
   };
   Boundary();
  };
  //Mochlos LMIB Final data used as a TAQ for the LMIB Late dataset of Myrtos-Pyrgos
 };


Options()
 {
  Resolution=1;
  Curve="intcal20.14c";
  kIterations=3000;
 };
 Plot()
 {
  //Data: Lespez et al. (2021)
  Outlier_Model("General",T(5),U(0,4),"t");
  Sequence()
  {
   Boundary();
   Phase("Malia Thera tsunami TAQ")
   {
    R_Date("Poz-96175 C22 charcoal",3200,30)
    {
     Outlier ("General",0.05);
    };
    R_Date("Poz-85442 C20 charcoal",3220,30)
    {
     Outlier ("General",0.05);
    };
    Date("Date Malia tsunami TAQ");
   };
   Boundary();
  };
 };
```

OxCal runfile for the Thera eruption dating model for Figure 8

```
Options()
 {
  Resolution=1;
  Curve="intcal20.14c";
  kIterations=3000;
 };
 Plot()
 {
  Sequence()
  {
   Boundary("STO");
   Sequence()
   {
    R_Date("Hd-23599-24426 'rings' 1-13",3383,11);
    R_Date("Hd-23587 'rings' 14-37",3372,12);
    R_Date("Hd-23589 'rings' 38-59",3349,12);
    R_Date("Hd-23588-24402 'rings' 60-72",3331,10);
   };
   Boundary("ETO");
  };
  Sequence("Therasia olive sample 88-3")
```

```
{
 Boundary();
 Sequence()
 {
  R_Date("AA111457 88-3 Inner",3314,23);
  R_Date("AA110275 88-3 Outer",3297,23);
 };
 Boundary();
};
Sequence("Therasia olive sample 88-2")
{
 Boundary();
 Sequence()
 {
  R_Date("AA110272 88-2 Inner",3361,21);
  R_Date("AA110273 88-2 Outer",3341,23);
  R_Date("AA110274 88-2 Bark",3301,23);
 };
 Boundary();
};
Sequence("Therasia olive sample 88-1")
{
 Boundary();
 Sequence()
 {
  R_Date("AA111456 88-1 Inner",3398,21);
  R_Date("AA110271 88-1 Outer",3320,22);
 };
 Boundary();
};
Sequence("Therasia olive sample 72-2")
{
 Boundary();
 Sequence()
 {
  R_Date("AA111458 72-2 Inner",3358,23);
  R_Date("AA111459 72-2 Outer",3342,24);
 };
 Boundary();
};
Sequence()
{
 Tau_Boundary("T");
 Phase("End Boundary/Outer/Bark Dates for Thera Eruption")
 {
  Date("=ETO");
  Date("=AA110275 88-3 Outer");
  Date("=AA110274 88-2 Bark");
  Date("=AA110271 88-1 Outer");
  Date("=AA111459 72-2 Outer");
 };
 Boundary("Eruption");
};
Sequence ("Sofular Cave")
{
 Boundary();
 Combine("Sofular Br and Mo immediate eruption tracers")
 {
  C_Date("Br",-1621,25);
  C_Date("Mo",-1617,25);
  Date("=Eruption");
 };
 Boundary();
```

```
  };
  Difference("D1","ETO","STO",U(0,72));
  Difference("D2","AA110275 88-3 Outer","AA111457 88-3 Inner",U(0,10));
  Difference("D3","AA110274 88-2 Bark","AA110272 88-2 Inner",U(0,79));
  Difference("D4","AA110271 88-1 Outer","AA111456 88-1 Inner",U(0,37));
  Difference("D5","AA111459 72-2 Outer","AA111458 72-2 Inner",U(0,50));
  Tau=(Eruption-T);
  Tau&=LnN(ln(3),ln(2));
 };

//Sofular Cave dates for the Br and Mo peaks from Badertscher et al. (2014)
//In Options, change Resolution=1; to Resolution=5; for the 5-year resolution model
```

Data employed and OxCal runfile for the models reported in Figure 9

```
Options()
 {
  Resolution=1;
  Curve="intcal20.14c";
  kIterations=3000;
 };
 Plot()
 {
  Sequence()
  {
   Boundary("STO");
   Sequence()
   {
    R_Date("Hd-23599-24426 'rings' 1-13",3383,11);
    R_Date("Hd-23587 'rings' 14-37",3372,12);
    R_Date("Hd-23589 'rings' 38-59",3349,12);
    R_Date("Hd-23588-24402 'rings' 60-72",3331,10);
   };
   Boundary("ETO");
  };
  Sequence("Therasia olive sample 88-3")
  {
   Boundary();
   Sequence()
   {
    R_Date("AA111457 88-3 Inner",3314,23);
    R_Date("AA110275 88-3 Outer",3297,23);
   };
   Boundary();
  };
  Sequence("Therasia olive sample 88-2")
  {
   Boundary();
   Sequence()
   {
    R_Date("AA110272 88-2 Inner",3361,21);
    R_Date("AA110273 88-2 Outer",3341,23);
    R_Date("AA110274 88-2 Bark",3301,23);
   };
   Boundary();
  };
  Sequence("Therasia olive sample 88-1")
  {
   Boundary();
   Sequence()
   {
```

```
    R_Date("AA111456 88-1 Inner",3398,21);
    R_Date("AA110271 88-1 Outer",3320,22);
   };
   Boundary();
  };
  Sequence("Therasia olive sample 72-2")
  {
   Boundary();
   Sequence()
   {
    R_Date("AA111458 72-2 Inner",3358,23);
    R_Date("AA111459 72-2 Outer",3342,24);
   };
   Boundary();
  };
  Sequence()
  {
   Tau_Boundary("T");
   Phase("End Boundary/Outer/Bark Dates for Thera Eruption")
   {
    Date("=ETO");
    Date("=AA110275 88-3 Outer");
    Date("=AA110274 88-2 Bark");
    Date("=AA110271 88-1 Outer");
    Date("=AA111459 72-2 Outer");
   };
   Boundary("Eruption");
  };
  Sequence("2/3 to 5")
  {
   Tau_Boundary ("S2/3");
   Phase ("Akrotiri secure Stages 2/3 Food Products or associated insect pest in
use/storage")
   {
    R_Date("OxA-1552 Lathyrus sp.",3390,65);
    R_Date("OxA-1555 Lathyrus sp.",3245,65);
    R_Date("OxA-1548 Lathyrus sp.",3335,60);
    R_Date("OxA-1549 Lathyrus sp.",3460,80);
    R_Date("OxA-1550 Lathyrus sp.",3395,65);
    R_Date("OxA-1553 Lathyrus sp.",3340,65);
    R_Date("OxA-1554 Lathyrus sp.",3280,65);
    R_Date("OxA-1556 Hordeum sp.",3415,70);
    R_Date("K-5352 pulses",3310,65);
    R_Date("K-3228 pulses",3340,55);
    R_Date("OxA-11817 ?Lathyrus sp.",3348,31);
    R_Date("OxA-11818 Hordeum sp.",3367,33);
    R_Date("OxA-11820 Hordeum sp.",3400,31);
    R_Date("OxA-11869 Hordeum sp.",3336,34);
    R_Date("OxA-12170 ?Lathyrus sp.",3336,28);
    R_Date("OxA-12171 Hordeum sp.",3372,28);
    R_Date("OxA-12175 Hordeum sp.",3318,28);
    R_Date("OxA-12172 Hordeum sp.",3321,32);
    R_Date("VERA-2756 Hordeum sp.",3317,28);
    R_Date("VERA-2757 ?Lathyrus sp.",3315,31);
    R_Date("VERA-2758 Hordeum sp.",3339,28);
    R_Date("VERA-2757 repeat ?Lathyrus sp.",3390,32);
    R_Date("VERA-2758 repeat Hordeum sp.",3322,32);
    R_Date ("OxA-25176 insect chitin",3368,29);
    R_Date("Hd-7092-6795 peas",3360,60);
   };
   Boundary("E2/3");
   Interval("Very Short Interval End Stages 2/3 to Stage 5 and
Eruption",LnN(ln(0.75),ln(3)));
```

```
   Boundary("=Eruption");
  };
  Difference("D1","ETO","STO",U(0,72));
  Difference("D2","AA110275 88-3 Outer","AA111457 88-3 Inner",U(0,10));
  Difference("D3","AA110274 88-2 Bark","AA110272 88-2 Inner",U(0,79));
  Difference("D4","AA110271 88-1 Outer","AA111456 88-1 Inner",U(0,37));
  Difference("D5","AA111459 72-2 Outer","AA111458 72-2 Inner",U(0,50));
 };

//for the alternative model change the Interval line above to:
// Interval("Short Interval End Stages 2/3 to Stage 5 and Eruption",LnN(ln(3),ln(2)));
```